Efficient Compression of CT Images with Modified Branched Inverse Pyramidal Decomposition

ROUMEN KOUNTCHEV
Department of Radio Communications
Technical University of Sofia
Bul. Kl. Ohridsky 8, Sofia 1000
BULGARIA
rkountch@tu-sofia.bg
http://www.tu-sofia.bg

ROUMIANA KOUNTCHEVA
T&K Engineering
Mladost 3
Pob 12
Sofia 1712
BULGARIA
kountcheva_r@yahoo.com

Abstract: - In the paper is presented one novel approach for adaptive compression of groups of computer tomography (CT) images, based on modified branched inverse pyramid decomposition. In result is obtained high compression ratio with retained image quality. To achieve this, was used the high correlation between sequences of CT images, representing same object(s). For the processing of a group of CT images was used the Inverse Pyramid Decomposition (IPD), with a special Branched structure, called Modified BIPD. The experimental results confirmed the efficiency of the presented method. The general characteristics of the new decomposition are a reliable basis for its successful use in various application areas for processing of similar (multi-view) or sequences of similar images. As it was proved by the experiments, this compression is very efficient when used for archiving of sequences of CT images. It could also be used for compression of still multispectral, hyper spectral or multi-view images and video sequences, obtained from surveillance video cameras, supersound scanners, thermo-vision systems, scanning microscopes, etc.

Key-Words: - Image processing, Archiving of CT images, Compression of sequences of medical images; Image group coding, Modified branched pyramidal image decomposition.

1 Introduction

Electronic healthcare records are important part of medical diagnostics and healthcare. As it is well-known, the old practice was based on paper rectors, which have significant disadvantages, related to legibility, resistance to humidity, accessibility, etc., etc. The contemporary approach is based on electronic rectors, which offer significant advantages, especially when visual medical data is concerned. This comprises various X-ray or ultrasound images, electrocardiograms, and many more. Computed tomography (CT) is one of the main contemporary diagnostic procedures. It uses special x-ray equipment to obtain cross-sectional pictures of the body, and for this, usually sequences of images for every patient are created and used. Important stage in CT is archiving the images obtained in an efficient manner concerning the data volume occupied and the image quality. A vast number of medical image compression techniques already exist [1-3,7,21,26], which can be divided into two large groups – lossless [4,9] and lossy [5,6] depending on the ability to restore the image fully or not. In both groups some type of image decomposition is used (for example, linear orthogonal transform or a wavelet one combined with spectral coefficients rearrangement and entropy coding).

The most famous file format, used for medical images archiving is DICOM [8,22], which is based on the JPEG standard. In [14] is proposed one approach based on adaptive sampling of DCT coefficients. The quality of the restored images after this compression is comparable to that of the JPEG2000 as the author shows, while the JPEG coder produces images with PSNR between 31 and 40 dB for same levels (i.e. visually lossless). In [5] authors confirm that wavelet decomposition assures better quality for the compressed images being than the JPEG-based coder.

Some resent publications emphasize the advantages of the wavelet decomposition for medical image compression combined with other techniques in order to construct more efficient coders (for example, using joint statistical characterization [1], by linear prediction of the spectral coefficients [13],

introducing region of interest (ROI) [6], incorporating planar coding [12], etc). Nevertheless the higher compression levels achieved, there is also reported significant reduction of the visual quality of these images [9,10]: while cumulative quality measures such as PSNR stay high the smoothing of vast image areas due to the wavelet coefficients quantization becomes intolerable for higher compression ratios.

In this paper is proposed one new approach for lossy compression of sequences of CT images with retained visual quality. It is based on linear orthogonal transforms using a type of spectral coefficients hierarchical grouping, provided by the Branched Inverse Pyramidal Decomposition (BIPD). Along with entropy coding this approach assures higher image quality than the previously developed methods at the same compression ratio (CR).

The paper is arranged as follows: in Section 2 are given the basics of the Branched Inverse Pyramid; Section 3 is devoted to representation of CT image sequences through Modified BIPD; in Section 4 are presented some experimental results, and in Section 5 are the Conclusions.

2 Basics of the Branched Inverse Pyramid Decomposition (BIPD)

The Inverse Pyramid decomposition is aimed at the efficient compression of still digital images. The digital image is represented by a matrix of size $(2^n m)\times(2^n m)$. For the processing, the matrix is first divided into blocks of size $2^n\times 2^n$ and on each is applied *Inverse Pyramid Decomposition* (IPD) [11]. It is performed as follows: on the matrix [*B*] of each block is applied pre-selected "truncated" orthogonal transform (TOT) and are calculated the values of relatively small number of "retained" coefficients, located in the high-energy area of the so obtained transformed (spectrum) matrix $[S_0]$, for example, these are usually the coefficients with spatial frequencies (0,0), (0,1), (1,0) and (1,1). After inverse orthogonal transform (IOT) of the "truncated" spectrum matrix $[\hat{S}_0]$, which contains the retained coefficients only, is obtained the matrix $[\hat{B}_0]$ for the initial (zero) IPD level (*p=0*), which approximates the matrix [*B*]. The accuracy of the approximation depends on: the positions of the retained coefficients in the matrix $[S_0]$; the values, used to substitute the missing coefficients from the approximating matrix $[\hat{S}_0]$ for the zero level, and the selected orthogonal transform (DCT, WHT, CHT, KLT, etc.). In the next (first) IPD level (*p=1*) is calculated the difference matrix $[E_0]=[B]-[\hat{B}_0]$. The result is then split into 4 similar sub-matrices of size $2^{n-1}\times 2^{n-1}$ and on each is applied the corresponding TOT. The total number of retained coefficients for the level *p=1* is 4 times larger than that in the zero level. In case, that the for this level is used the Walsh-Hadamard transform, the values of coefficients (0,0) in the IPD decomposition levels 1 and higher are always equal to zero, which permits to reduce the number of retained coefficients with ¼. On each of the 4 spectrum matrices $[\hat{S}_1]$ for the IPD level *p=1* is applied IOT and in result are obtained 4 corresponding sub-matrices, which build the approximating difference matrix $[\hat{E}_0]$. In the next IPD level (*p=2*) is calculated the difference matrix $[E_1]=[E_0]-[\hat{E}_0]$. After that each difference sub-matrix is divided in similar way as in level 1, into 4 matrices of size $2^{n-2}\times 2^{n-2}$; for each is performed TOT, etc. The maximum possible number of decomposition levels for one image is *n* (for *p = n-1*). In this case the total number of "retained" coefficients for all levels ($4m^2+3.4m^2+.....+3.4^{n-1}m^2 = 4^n m^2$) is equal to the number of pixels in the image, and hence, the IPD is not "overcomplete". In the last (highest) IPD level is obtained the "residual" difference matrix. In case that the image should be losslessly coded, each block of the residual matrix is processed with full orthogonal transform and no coefficients are omitted.

The Branched IPD is enhanced version of IPD. For this, the IPD was modified for processing of a group of related images. In this case, the first approximation calculated for the lowest level of the pre-selected reference image is used by the remaining images in the group when their next approximations are calculated. It is represented by the Block diagram shown on Fig. 1. The IPD for each block from the reference image, called "Main Pyramid" is of 3 levels (*n=3*, for *p=0,1,2*). The values of coefficients, calculated for these 3 levels, compose the inverse pyramid, whose sections are of different color each. The coefficients (*0,0*), (*0,1*), (*1,0*) and (*1,1*) in the level *p=0* from all blocks compose corresponding matrices of size m×m each, colored in yellow. These 4 matrices build the "Branch for level 0" of the Main Pyramid. Each is then divided into blocks of size $2^{n-1}\times 2^{n-1}$, on which in similar way are build corresponding 3-level IPDs (*p=00,01,02*). The retained coefficients (*0,1*), (*1,0*) and (*1,1*) in the level *p=1* of the Main Pyramid from all blocks build matrices of size $2^m\times 2^m$ (colored in pink). Each such matrix is divided into blocks of size $2^{n-1}\times 2^{n-1}$, on which in similar way are build corresponding 3-level IPDs (*p=10,11,12*). The

retained coefficients, calculated after TOT from the blocks of the Residual Difference in the last level (*p=2*) of the Main Pyramid, build matrices of size *4m×4m*; from the first level (*p=00*) of the "Branch Pyramid 0" - matrices of size ($m/2^{n-1}\times m/2^{n-1}$); and from the frst level (*p=10*) of the "Branch Pyramid 1" - matrices of size ($m/2^{n-2}\times m/2^{n-2}$).

In order to reduce the correlation between elements from the so obtained matrices, on each group of 4 spatially neighboring elements is applied the following transform: the first one is substituted by their average value, and each of the remaining 3 – by its difference to next elements, scanned counter clockwise. The coefficients, obtained this way from all levels of the Main and Branch Pyramids are arranged in one-dimensional sequences in accordance to Peano-Hilbert scan and after that are quantizated and entropy coded using Adaptive RLC and Huffman. The values of the spectrum coefficients are quantizated only in case that the image coding is lossy. In order to retain the visual quality of the restored images, the quantization values are related to the sensibility of the human vision to errors in different spatial frequencies. For the reduction of these errors, together with retained compression efficiency, in the consecutive BIPD levels could be used various fast orthogonal transforms: for example, in the zero level could be used DCT, and in the next levels - WHT.

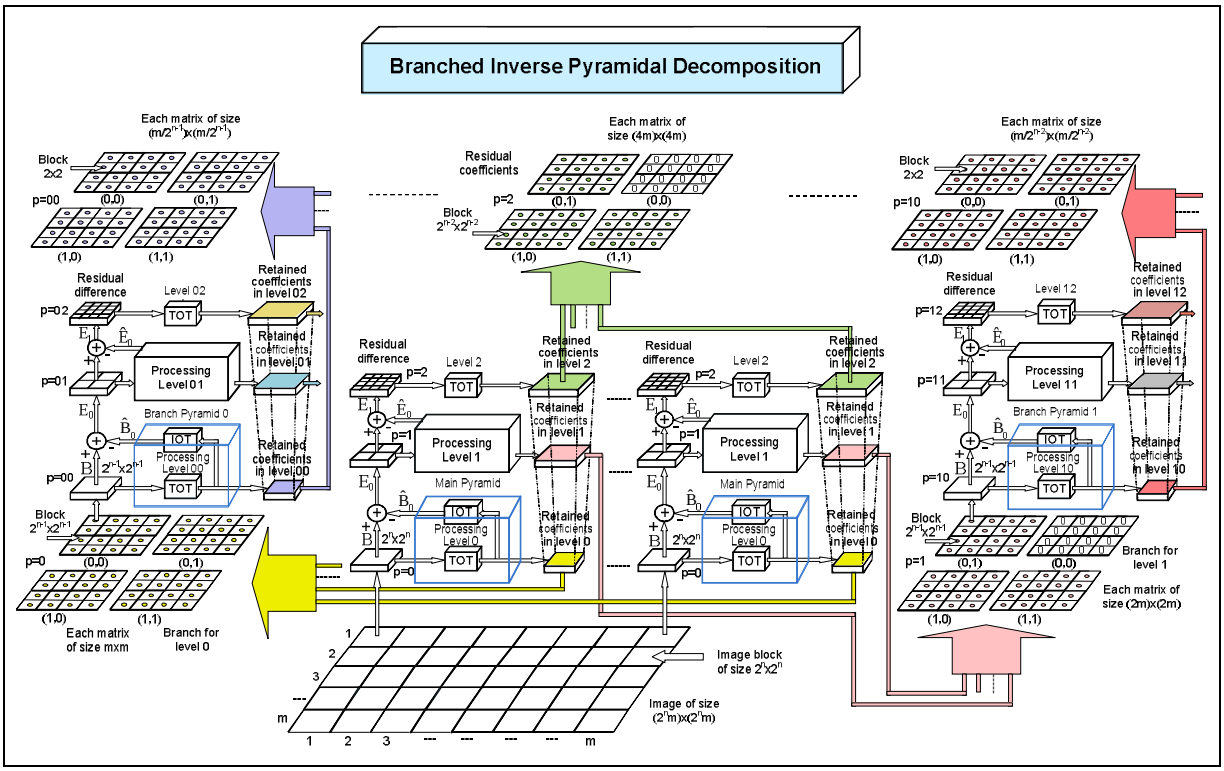

Fig. 1. Block diagram of Branched Inverse Pyramidal Decomposition

The decoding of the compressed image data is done, performing the already described operations in inverse order.

The basic quality of the BIPD is that it permits to achieve significant decorrelation of the processed image data. In result, the BIPD permits the following:

- To achieve highly efficient compression with retained visual quality of the restored image (i.e. visually lossless coding), or efficient lossless coding, depending on the application requirements;
- Layered coding and transfer of the image data, in result of which is obtained low transfer bit-rate with gradually increased quality of the decoded image;
- Lower computational complexity than that of the wavelet decompositions;
- Easy adaptation of the coder parameters, so that to ensure the needed concordance of the so obtained data stream, to the ability of the communication channel;

- Resistance to noises in the communication channel, or due to compression/decompression. The reason for this is the use of TOT in the decoding of each image block;
- Retaining the quality of the decoded image unchanged after multiple codings/decodings;

The BIPD could be further developed and modified in accordance to requirements of various possible applications. One of these applications for processing of groups of similar images (in this case, a sequence of Computer tomography images) is given below.

3 Representation of CT Image Sequences through Modified BIPD

For the Modified BIPD coding is used the high similarity between group of CT images of same object. Based on this, images in one group are coded together (Group coding). In order to make the information redundancy in the sequence of matrices $[B_n]$ for $n = -N,-N+1,..,-1,0,1,..,M-1,M$ smaller, here is offered to use the following modification of the image decomposition (the relations below are for decomposition of 2 levels only).

2.1 Reference Image Selection in the Groups of CT images

First, one of the images in the group is selected to be used as a reference. The image which will be chosen to be used as a reference is selected on the basis of the histogram analysis: the CT image, whose histogram is closest to all remaining images in the processed group, is selected to be the reference. The analysis is made using the correlation coefficient. The correlation coefficient ρ_{xy} between vectors $\vec{X} = [x_1, x_2, ..., x_m]^t$ and $\vec{Y} = [y_1, y_2, ..., y_m]^t$, which represent the histograms of the two images is [16]:

$$\rho_{x,y} = \sum_{i=1}^{m}(x_i - \bar{x})(y_i - \bar{y}) \Big/ \left(\sqrt{\sum_{i=1}^{m}(x_i - \bar{x})^2}\right)\left(\sqrt{\sum_{i=1}^{m}(y_i - \bar{y})^2}\right) \quad (1)$$

where $\bar{x} = \frac{1}{m}\sum_{i=1}^{m} x_i$ and $\bar{y} = \frac{1}{m}\sum_{i=1}^{m} y_i$

are the mean values of the two histograms and m is the number of brightness levels for the two CT images. The decision for the reference image selection is taken after the histograms of the CT images had been calculated and then the correlation coefficients for all couples of histograms are calculated and evaluated.

For group of $(N+M+1)$ CT images the number of these couples $l(p,q)$ is:

$$L = \sum_{p=1}^{N+M}\sum_{q=p+1}^{N+M+1} 1(p,q), \quad (2)$$

When all L coefficients ρ_{pq} are calculated, is defined the index p_0 in $\rho_{p_0 q}$, for which is satisfied the requirement:

$$\sum_{q=1}^{N+M+1} \rho_{p_0 q} \geq \sum_{q=1}^{N+M+1} \rho_{pq} \quad \text{for } p, q = 1,2,..,N/M, \quad (3)$$

when $p \neq q$ and $p \neq p_0$.

From this follows, that the reference image should be $[B_R] = [B_{p_0}]$. Each block of the n^{th} CT image is represented by the matrix $[B_n]$ of size $2^m \times 2^m$, when $n=-N,-N+1,..,-1,0,1,...,M-1,M$. Besides, the matrix $[B_0]$ corresponds to the "reference" image, placed in the position $n=0$ of the sequence $[B_n]$. In order to reduce the information redundancy, contained in the sequence of matrices $[B_n]$, is used IPD modification of 2 levels only [17]:

2.2 Coding Groups of CT images with Modified IPD:

1. For IPD level $p=0$ is calculated the transform $[S_0^0]$ of the reference image $[B_0]$ with direct orthogonal transform:

$$[S_0^0] = [T_0][B_0^0][T_0], \quad (4)$$

where $[T_0]$ is the matrix of the used direct orthogonal transform, of size $2^m \times 2^m$.

2. The matrix of the approximated reference image is calculated:

$$[\hat{S}_0^0] = [m_0(u,v)s_0^0(u,v)], \quad (5)$$

where $m_0(u,v)$ is the element of the matrix-mask $[M_0]$, used to define the retained transform coefficients

$$m_0(u,v) = \begin{cases} 1, \text{if } s_0^0(u,v) \text{ - retained coefficient,} \\ 0 \quad \text{- in all other cases,} \end{cases} \quad (6)$$

3. The approximated reference image $[\hat{B}_0]$ is calculated through inverse orthogonal transform:

$$[\hat{B}_0] = [T_0]^t[\hat{S}_0^0][T_0]^t, \quad (7)$$

where $[T_0]^t=[T_0]^{-1}$ is the matrix of the inverse orthogonal transform, of size $2^m \times 2^m$.

4. The difference matrix is calculated in accordance with the relation below:

$$[E_0]=[B_0]-[\hat{B}_0] \quad (8)$$

The difference matrix is then divided into 4 sub-matrices:

$$[E_0]=\begin{bmatrix}[E_0^1] & [E_0^2]\\ [E_0^3] & [E_0^4]\end{bmatrix}, \quad (9)$$

where $[E_0^i]$ for $i=1,2,3,4$ are sub-matrices of size $2^{m-1} \times 2^{m-1}$.

5. For IPD level $p=1$ is calculated the transform $[S_0^i]$ of the i^{th} sub-matrix of the difference $[E_0]$, using the direct orthogonal transform:

$$[S_0^i]=[T_1][E_0^i][T_1] \text{ for } i=1,2,3,4, \quad (10)$$

where $[T_1]$ is the matrix of the direct orthogonal transform, of size $2^{m-1} \times 2^{m-1}$.

6. The approximated i^{th} transform is calculated:

$$[\hat{S}_0^i]=[m_1(u,v)\, s_0^i(u,v)], \quad (11)$$

where $m_1(u,v)$ is the element of the matrix-mask $[M_1]$ used to define the retained spectrum coefficients:

$$m_1(u,v)=\begin{cases}1, \text{if } s_0^i(u,v) \text{ - retained coefficient,}\\ 0 \quad \text{- in all other cases,}\end{cases} \quad (12)$$

7. For the level $p=1$ of the multi-view image $[B_n]$ decomposition is calculated the difference:

$$[E_n]=[B_n]-[\hat{B}_0] \quad (13)$$

for $n = -N,-N+1,..-1,0,1,..,M-1,M$.

The so calculated difference is then split into 4 sub-matrices:

$$[E_n]=\begin{bmatrix}[E_n^1] & [E_n^2]\\ [E_n^3] & [E_n^4]\end{bmatrix}, \quad (14)$$

where $[E_n^i]$ for $i = 1,2,3,4$ are sub-matrices of size $2^{m-1} \times 2^{m-1}$.

8. The i^{th} transform $[S_n^i]$ of the difference sub-matrix $[E_n^i]$ is calculated, using direct orthogonal transform:

$$[S_n^i]=[T_1][E_n^i][T_1] \text{ for } i=1,2,3,4 \quad (15)$$

9. The approximated i^{th} transform (i.e., the spectrum of the difference matrix $[E_n^i]$) is calculated:

$$[\hat{S}_{0n}^i]=[m_1(u,v)\, s_{0n}^i(u,v)], \quad (16)$$

where $m_1(u,v)$ is the element of the matrix-mask used to define the retained spectrum coefficients.

10. The difference matrices of the approximated transforms are calculated:

$$[\Delta\hat{S}_n^i]=[\hat{S}_0^i]-[\hat{S}_n^i] \quad (17)$$

for $n = -N,-N+1,..-1,0,1,..,M-1,M$.

11. The coefficients of matrices $[\hat{S}_0^0]$ and $[\Delta\hat{S}_0^i]$ *for* $i=1,2,3,4$ and $n=-N,-N+1,..,-1,0,1,..,M-1,M$ in decomposition levels $p=0,1$ of the corresponding $(N+M+1)$ pyramids are losslessly coded.

2.3 Decoding Groups of CT images with Modified IPD:

1. The losslessly coded coefficients of spectrum matrices $[\hat{S}_0^0]$ and $[\Delta\hat{S}_0^i]$ for $i=1,2,3,4$ and $n=-N,-N+1,..,-1,0,1,..,M-1,M$ in levels $p=0,1$ of the corresponding $(N+M+1)$ pyramids are decoded;

2. The approximated transforms in the decomposition level $p=1$ are restored:

$$[\hat{S}_n^i]=[\hat{S}_0^i]+[\Delta\hat{S}_n^i] \quad (18)$$

for $n = -N,-N+1,..,-1,0,1,..,M-1,M$.

3. For the reference image ($n=0$) is calculated each i^{th} approximated sub-matrix $[\hat{E}_0^i]$ of the difference matrix $[\hat{E}_0]$, using the inverse 2D orthogonal transform:

$$[\hat{E}_0^i]=[T_1]^t[\hat{S}_0^i][T_1]^t \text{ for } i=1,2,3,4, \quad (19)$$

4. The matrix of the approximated reference image $[\hat{B}_0]$ for the level $p=0$ is calculated, using the corresponding inverse orthogonal transform:

$$[\hat{B}_0]=[T_0]^t[\hat{S}_0^0][T_0]^t \ , \quad (20)$$

5. The matrix $[\hat{B}]$ of the restored reference image ($n=0$) is calculated:

$$[\hat{B}]=[\hat{B}_0]+[\hat{E}_0] \ . \quad (21)$$

6. The difference sub-matrices $[\hat{E}_n^i]$ for $i=1,2,3,4$ of the multi-view images for the IPD level $p=1$ are calculated through corresponding inverse orthogonal transform:

$$[\hat{E}_n^i]=[T_1]^t[\hat{S}_n^i][T_1]^t \quad (22)$$

for $n=-N,-N+1,..,-1,0,1,..,M-1,M$.

7. The corresponding matrices $[\hat{B}_n]$ of the restored multi-view images are calculated:

$$[\hat{B}_n]=[\hat{E}_n]+[\hat{B}_0] \quad (23)$$

for $n = -N,-N+1,..,-1, 1,..,M-1,M$.

In similar way are decoded the matrices $[\hat{B}_n]$ of all blocks of size $2^m \times 2^m$, which build the CT images, for $n = -N, -N+1,.., -1, 0, 1,., M-1, M$. The difference between the basic IPD, and the modification, used for the processing in the decoding, is represented by Eqs. (18) and (23). Here, the restoration of the reference CT image is performed in the way as it is done in the basic IPD, i.e. the two approximations are used directly for the creation of the reference image, and the remaining images in the same sequence are restored using the coarse approximation for the reference image and the fine approximation, belonging to the corresponding image.

Besides, in the modified approach, presented here, all images use the same coarse approximation, and in the second decomposition level each image is processed individually. Another significant difference is that the basic IPD decomposition usually comprises 3 or 4 levels, starting with large image sub-blocks. The modification, used for the group representation, is based on 2-level decomposition, built for relatively small sub-blocks, usually of size 8×8 pixels for the lower level and 4×4 pixels – for the higher one. The block diagram of the Modified Branched 2-level IPD, used for coding of one sub-group of CT images is shown on Fig. 2. The decoding is performed in reverse order.

In a group of medical CT images used for this processing, the first in the sequence is used as a reference. In case that the sequence contains large number of images, best results are obtained if the sequence is divided into groups of 5 or 6 consecutive images (the mutual correlation becomes lower for larger number of consecutive images in the group).

Here is used two-dimensional Truncated Orthogonal Transform (2D-TOT), whose retained sets of coefficients are defined by the "ones" in the binary matrices-masks $[M_0]$ and $[M_1]$ used respectively for decomposition levels $p = 0,1$. For each sub-group of CT images the lossless compression in the last stage of the processing comprises run-length coding (RLC), Huffman coding (HC) and arithmetic coding (AC).

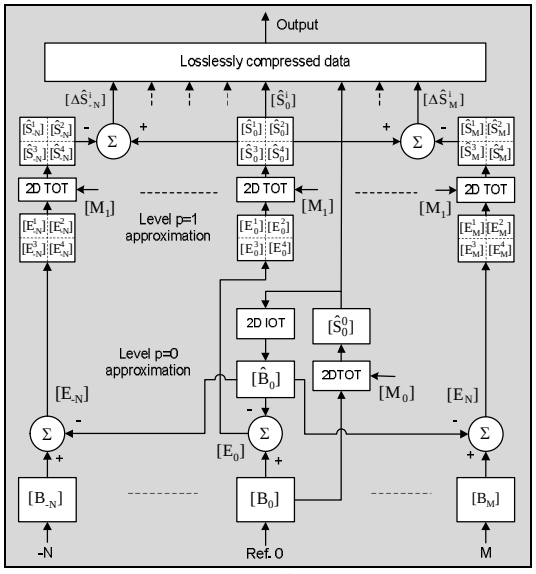

a. Coder

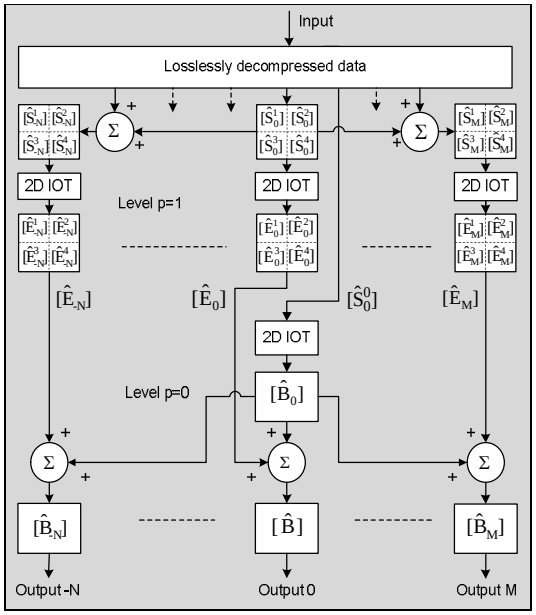

b. Decoder

Fig.2. Block diagram of the 2-level Modified BIPD coder/decoder for $(N+M+1)$ CT images

The block diagram represents the processing of one sub-block of the processed image only. The group coding for color images is performed in a similar way, but it requires each color component to be processed individually. Depending on the color format (RGB, YUV, YC_RC_B, KLT, etc.), and the color sampling format (4:4:4, 4:2:0, 4:1:1, etc.) for each component is built an individual pyramid. The approach based on the processing of the reference image and the remaining ones in the group, is retained.

4 Experimental results

The software implementation of the new approach for Group compression, presented above, confirmed its efficiency.

For the experiments were used images from the image database of the Medical University and Technical University in Sofia. The CT test images used for the experiments given below, were a group of 576 grayscale slices in DICOM format, of size *512×512* pixels each, with intensity depth of 16 bpp.

On Fig. 3.a is presented graphically the correlation coefficient between each two images from the group of 560 images, and on Fig. 3.b – the correlation coefficient between the first image and all the others. As suggested before, a strong variation of the correlation exists inside a candidate group around a proper reference and outside it asymptotically goes to a constant value.

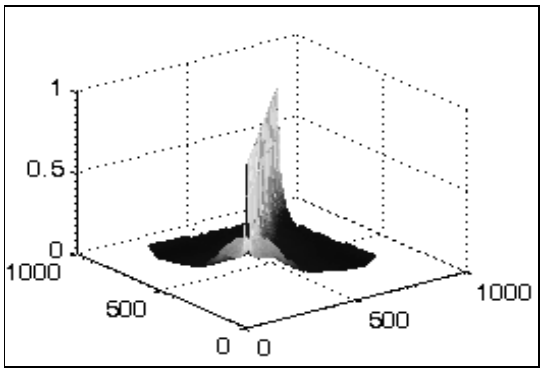

a

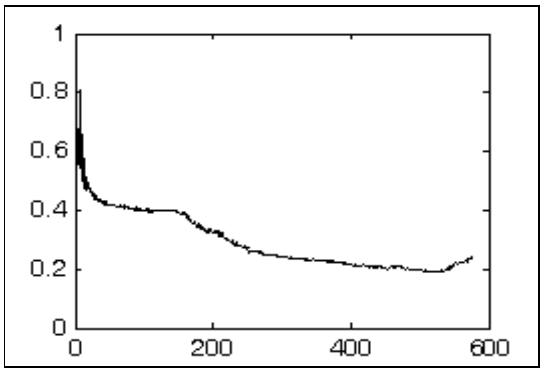

b

Fig. 3. Graphic presentations for the correlation for: a) all couples of images; b) the first and all others

One test group consisting of 9 images is shown on Fig. 4: the first image was selected to be used as a reference. The size of the initial sub-block was *16×16* (*n=4*). In the zero and first level of the branch, the retained coefficients were 4, placed in the low-frequency area. For the main branch of the inverse pyramid in the first and second level, the same 4 low-frequency coefficients were retained.

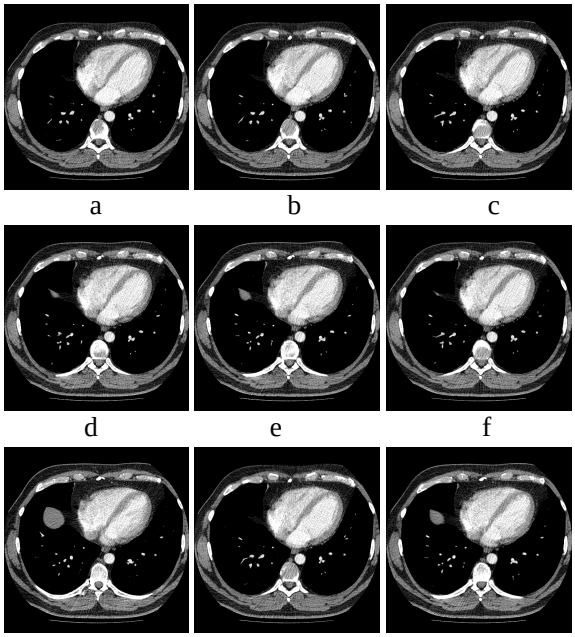

a b c

d e f

g h i

Fig. 4. Test group of 9 images: a) the reference image, (b-i) – the remaining 8 images of same group

In Table 1 are given the results obtained for 5 test images with MBIPD coding (Group Coding, GC) and comparison with the JPEG standard. For the experiments was used the software implementation of the method in Visual C. It is noticeable, that for approximately same quality the compression ratio (CR) is higher for the MBIPD (Group coding). Besides, for similar quality obtained through JPEG 2000, the visual quality of MBIPD is better, because the JPEG 2000 decreases the small details (in result of the use of wavelet transform).

Table 1. Results obtained for 5 test images.

Image	CR_{GC}	$PSNR_{GC}$	CR_{JPEG}	$PSNR_{JPG}$[dB]
a	68.30	31.84	47	31.88
b	51.89	31.88	46	31.76
c	47.28	31.76	46	31.78
d	46.28	31.51	46	31.91
e	43.10	31.37	43	32.44
Mean	51.37	31.67	45.6	31.95

In Table 2 are given the results obtained for a group of 9 CT images, using Group Coding of 3 levels. In this case, the image named “Image 1” from the tested Group was used as a reference. The processing was done under conditions given below:

The size of the initial sub-block was *16×16* (*n=4*); in the zero, first and level of the branch, the retained coefficients were 4, placed in the low-frequency area. For the main branch of the inverse pyramid in the first and second level, the same 4 low-frequency coefficients were retained.

The three main columns of Table 2 show the results obtained for each of the consecutive decomposition levels of BIPD (0,1,2). Columns CR give the Compression Ratio as bits-per-pixel (bpp); PSNR and SSIM [25] were used for evaluation of the quality of restored images.

As it is seen, the PSNR is getting lower when images with larger differences from the reference are processed, but the visual quality still remains high (more than 32 dB for the lowest level and higher for the next ones).

In fact, for images of such kind the SSIM represents very well the visual quality of the restored images and suits better the Human visual system. This is because of the different approach in both cases. As it is known, MSE or PSNR estimate perceived errors while SSIM considers image degradation as perceived change in structural information. Here the structural information represents the idea that processed pixels have strong inter-dependencies especially when they are spatially close. These dependencies carry important information about the structure of the objects in the visual scene. In medical images where there are no sharp transitions and the structure in most parts is similar, the approach based on the SSIM gives better results when visual image quality is concerned. Anyway, both PSNR and SSIM prove the better quality of highly compressed groups of medical CT images.

Table 2. Compression and quality for a group of test images at 3 levels of the main BIPD

Image	Level 0			Level 1			Level 2		
	CR (bpp)	PSNR (dB)	SSIM	CR (bpp)	PSNR (dB)	SSIM	CR (bpp)	PSNR (dB)	SSIM
1(Refer.)	0.12	38.37	0.9862	0.35	39.84	0.9935	1.33	44.16	0.9955
2(Diff.1)	0.10	37.86	0.9867	0.33	39.80	0.9941	1.32	43.38	0.9961
3(Diff.2)	0.10	35.53	0.9862	0.33	37.36	0.9937	1.33	43.12	0.9960
4(Diff.3)	0.11	35.16	0.9811	0.37	37.11	0.9875	1.44	42.55	0.9871
5(Diff.4)	0.11	35.75	0.9706	0.35	36.94	0.9953	1.39	41.98	0.9970
6(Diff.5)	0.10	34.12	0.9515	0.34	36.54	0.9650	1.38	41.35	0.9667
7(Diff.6)	0.12	33.13	0.9501	0.44	35.27	0.9612	1.74	40.83	0.9669
8(Diff.7)	0.12	33.35	0.9487	0.44	35.12	0.9523	1.75	40.56	0.9675
9(Diff.8)	0.12	32.01	0.9401	0.43	34.86	0.9594	1.73	40.10	0.9695

On Fig. 5 is given the graphic representation of the relation between the compression ratio and the quality of the restored image obtained after processing same groups of test CT images with BIPD and JPEG 2000.

For the comparison were used the PSNR and SSIM evaluation. It is easy to notice that in both cases the quality of the restored images for big compression ratios is higher for BIPD. For lower compression ratio the quality of the restored images is almost same for both methods.

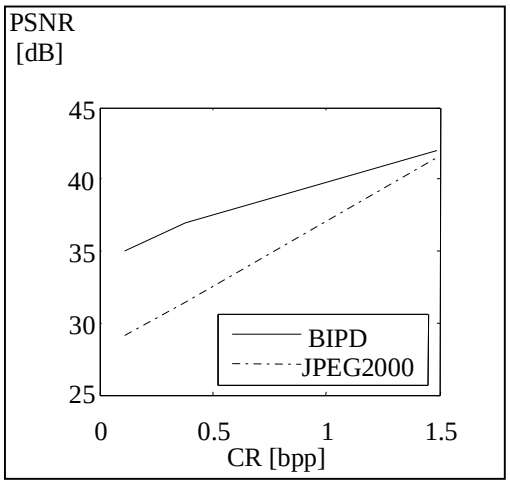

a

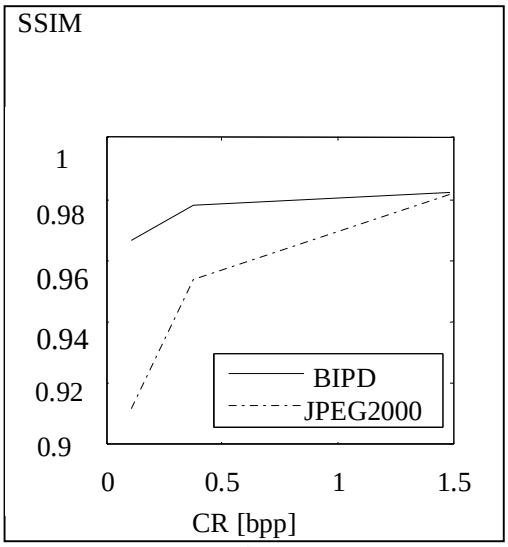

b

Fig. 5. Quality comparison between BIPD and JPEG2000 based on a) PSNR and b) SSIM.

On Fig. 6 is shown one of the test images after compression ratio 0.11 bpp obtained using the MBIPD and JPEG 2000 (a). There are also shown extracted enlarged parts of same test image. In spite of close PSNR values obtained for both cases, the visual quality of the restored image after BIPD is better than that of JPEG2000. It is noticeable, that significant parts of the JPEG image are fuzzy and the tissue structure is not clear, while the details in same parts of the BIPD image are retained much better.

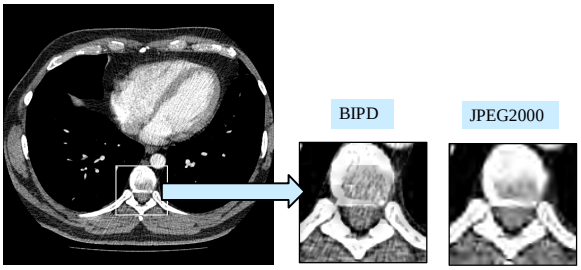

a b c

Fig. 6. Visual quality comparison for a segment of the: a) original referent CT image compressed at CR = 0.11 bpp, using b) MBIPD and c) JPEG2000.

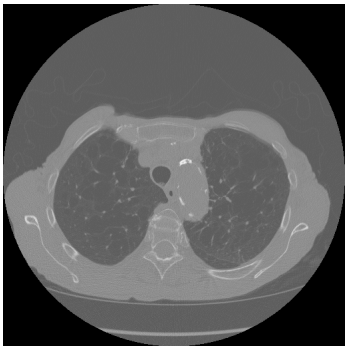

a. Original image

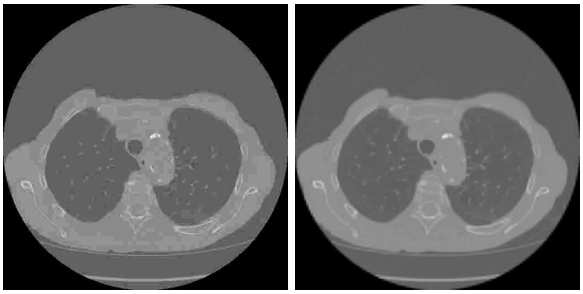

b. After JPEG c. After GC

Fig. 7. Restored images after approximately same compression (JPEG and GC)

On Fig. 7 are shown restored images after JPEG compression and Group coding (GC). The compression ratio for the JPEG image was CR = 46 and the corresponding PSNR was 31,76 dB; the compression ratio for the Group coding was CR = 51 and the PSNR in this case was 31,88 dB. In this case both the compression ratio and the image quality are higher for the GC. In the lower part of the JPEG image are noticeable even false brightness transitions, while such changes are not detectable in the GC image.

5 Conclusions

The main advantages of the presented new method for compression of sequences of medical CT images are:

- The higher visual quality obtained for same compression ratios;
- The comparatively low computational complexity (the computational complexity of the new method is comparable to that of the IPD method which was presented and evaluated in detail in [15]).

The general characteristics of the Modified BIPD are a reliable basis for its successful use in various application areas. As it was proved by the experiments, this compression is very efficient for archiving of sequences of CT images. It could also be used for compression of still multispectral, hyper spectral or multi-view images and video sequences [17], obtained from surveillance video cameras, super sound scanners, thermo-vision systems, scanning microscopes, i.e. – in all cases when still or slowly moving objects are concerned. The flexibility of the offered approach permits it to be used together with methods for image segmentation, depending on the application. Combined with tools for invariant object representation and feature description, same approach could be used for enhanced search-by-content in image databases [18,19,24]. In this case the search is performed for the reference image of the group only, which decreases significantly the

number of needed calculations. Some of these application areas had already been investigated and confirmed the expected results [18-20].

The investigation will be further developed through modeling and experiments and related to contemporary methods for image segmentation [23], object detection, etc., because these techniques become of high importance in the up-to-day medical diagnostics. For this will be used large image databases with medical images of various kinds. The so obtained results will be evaluated and compared to other similar algorithms and will be investigated possible new application areas: remote investigation of the earth surface from sequences of satellite photos, medical diagnostic, automatic manufacturing control, defense, etc.

Acknowledgement

This work was supported by the Joint Research Project: "Electronic Health Records for the Next Generation Medical Decision Support in Romanian and Bulgarian National Healthcare Systems", Contr. No. DNTS 02/09.

References:

[1] N. Hounsfield, Computed Medical Imaging: Nobel Lecture, Dec. 1979. *J. Computer Assist. Tomography*, Vol. 4: 665, 1980.

[2] H. Huang, R. Taira, Infrastructure Design of a Picture Archiving and Communication System, *American Journal of Roentgenology*, 1992, Vol. 158, pp. 743-749.

[3] R. Buccigrossi, E. Simoncelli, Image Compression via Joint Statistical Characterization in the Wavelet Domain. *IEEE Trans. on Image Processing*, 1999, Vol. 8, No.12, pp. 1688-1701.

[4] A. Clunie, Lossless Compression of Grayscale Medical Images - Effectiveness of Traditional and State of the Art Approaches. *Proc SPIE*, V. 3980, 2000, pp.74-84.

[5] B. Erickson, A. Manduca A. P. Palisson, K. Persons, F. Earnest, V. Savcenko, N. Hangiandreou, Wavelet Compression of Medical Images. *Radiology*, 1998, Vol. 206, pp. 599-607.

[6] S. Gokturk, C. Tomasi, B. Girod, C. Beaulieu, Medical Image Compression Based on Region of Interest, with Application to Colon CT Images. *Proc. of the 23rd Annual International Conference of the IEEE Engineering in Medicine and Biology Society*, 2001, vol. 3, pp. 2453 - 2456.

[7] K. Karadimitriou, J. Tyler, Min-max Compression Methods for Medical Image Databases. *ACM SIGMOD Record*, 1997, Vol. 26, pp. 47-52.

[8] R. Graham, R. Perriss, A. Scarsbrook, DICOM Demystified: A Review of Digital File Formats and their Use in Radiological Practice. *Clinical Radiology*, 2005, V. 60, pp. 1133-1140.

[9] J. Kivijarvi, T. Ojala, T. Kaukoranta, A. Kuba, L. Nyu´l, O. Nevalainen, A Comparison of Lossless Compression Methods for Medical Images. *Computerized Medical Imaging and Graphics*, 1998, Vol. 22, pp. 323–339.

[10] J. Ko, J. Chang, E. Bomsztyk, J. Babb, D. Naidich, H. Rusinek, Effect of CT Image Compression on Computer-assisted Lung Nodule Volume Measurement. *Radiology*, 2005, vol. 237, pp. 83–88.

[11] R. Kountchev, R. Kountcheva, Image Representation with Reduced Spectrum Pyramid. In: *New Directions in Intelligent Interactive Multimedia*, G. Tsihrintzis, M. Virvou, R. Howlett, L. Jain (Eds.), Springer, Berlin, 2008.

[12] Y. Lalitha, M. Latte, Image Compression of MRI Image Using Planar Coding. *International Journal of Advanced Computer Science and Applications*, 2011, vol. 2, No.7, pp. 23-33.

[13] S. Ramesh, D. Shanmugam, Medical Image Compression Using Wavelet Decomposition for Prediction Method. *International Journal of Computer Science and Information Security (IJCSIS)*, 2010, vol. 7, No.1, pp. 262-265.

[14] Y. Wu, Medical Image Compression by Sampling DCT Coefficients. *IEEE Trans. on Information Technology in Biomedicine*, 2002, Vol. 6, No.1, pp. 86-94.

[15] R. Kountchev, M. Milanova, C. Ford, R. Kountcheva, Multi-layer Image Transmission with Inverse Pyramidal Decomposition, In: *Computational Intelligence for Modeling and Predictions*, vol.2, Ch. 13, Springer, 2005, pp. 179–196.

[16] I. Bronshtein, K. Semendyayev, G. Musiol, H. Muehlig, *Handbook of Mathematics*, 5th ed., Springer, 2007.

[17] R. Kountchev, Vl. Todorov, R. Kountcheva. Compression of Multispectral and Multi-view Images with Inverse Pyramid Decomposition, *International Journal of Reasoning-based*

Intelligent Systems (*IJRIS)*, Vol. 3, No. 2, 2011, pp. 124-131.

[18] R. Kountchev, Vl.Todorov, R. Kountcheva. RSTC-Invariant Object Representation with Modified 2D Mellin-Fourier Transform. *WSEAS Trans. on Signal Processing*, Vol. 6, Iss. 4, October 2010, pp. 196-207.

[19] R. Kountchev, B. Iantovics, R. Kountcheva. Hierarchical Access Control and Content Protection in Medical Image Archives, Based on Inverse Pyramid Decomposition. *Proc. of the 10th WSEAS Intern. Conf. on Signal Processing, Robotics and Automation (ISPRA'11)*, Cambridge, UK, 2011, pp. 391-396.

[20] R. Kountchev, R. Kountcheva. One Approach for Decorrelation of Multispectral Images, Based on Hierarchical Adaptive PCA. *Proc. of the 12th WSEAS Int. Conf. on Signal Processing Computational Geometry and Artificial Vision (ISCGAV '12)*, Istanbul, Turkey, 2012, pp. 68-73.

[21] H. Costin, Cr. Rotariu, PET and CT images Registration by Means of Soft Computing and Information Fusion, *Proc. of 1st WSEAS Intern. Conf. on Biomedical Electronics and Biomedical Informatics (BEBI '08)*, Rhodes, Greece, August 20-22, 2008, pp. 150-161.

[22] M. Otesteanu, V. Gui, 3D Image Sensors, an Overview, *WSEAS Transactions on Electronics*, Vol. 5, Issue 3, 2008, pp. 53-56.

[23] M. Lascu, D. Lascu, A New Morphological Image Segmentation with Application in 3D Echographic Images. *WSEAS Transactions. on Electronics*, Vol. 5, Issue 3, 2008, pp. 72-82.

[24] A. Rövid, P. Várlaki, L. Szeidl, HOSVD Based Data Representation and LPV Model Complexity Reduction, *WSEAS Conf. on Applications of Mathematics and Computer Engineering*, USA, 2011 pp. 164-169.

[25] Z. Wang, A. Bovik, Mean Square Error: Love it or Leave it? IEEE Signal Processing Magazine, Jan. 2009, pp. 98-117.

[26] T. Acharya, P. Tsai, JPEG 2000 Standard for Image Compression: Concepts, Algorithms and VLSI Architectures, J. Wiley, 2005.